Supporting Information

Atomic differentiation of silver binding preference in protein targets: *Escherichia coli* malate dehydrogenase as a paradigm

Haibo Wang[a*], Xinming Yang[a], Minji Wang[a,b], Menglong Hu[c], Xiaohan Xu[a], Aixin Yan[d], Quan Hao[c], Hongyan Li[a] and Hongzhe Sun[a*]

[a]Department of Chemistry and CAS-HKU Joint Laboratory of Metallomics on Health and Environment, The University of Hong Kong, Hong Kong, P. R. China.

[b]School of Chemistry and Molecular Engineering, East China Normal University, No. 3663 Zhongshan Road North, Shanghai, 200062, P. R. China.

[c]School of Biological Sciences, The University of Hong Kong, Hong Kong, P. R. China.

[d]School of Biomedical Sciences, The University of Hong Kong, Laboratory Block, 21 Sassoon Road, Pokfulam, Hong Kong, P. R. China.

* Correspondence should be addressed to H. Wang (haibo_wang@connect.hku.hk) and H. Sun (hsun@hku.hk).

Table of Contents

Materials and experimental design

Materials

E. coli K12 MG 1655 is from our lab collection. The FPLC system was purchased from GE Healthcare. The column gel electrophoresis separation system was home-built by modifying a commercially available Mini Prep Cell system (Bio-Rad). Inductively coupled plasma mass spectrometry (ICP-MS) detections were performed on the Agilent 7700× system. All chemical reagents and standard proteins were purchased from Sigma-Aldrich unless otherwise specified. The malate dehydrogenase activity assay kit was purchased from Abcam. All solutions were prepared from Milli-Q water (Milli-Q Ultrapure water systems, Millipore).

DNA manipulation and plasmid construction

The strains, plasmids and primers used for protein overexpression are listed in Table S1 and S2. The *E. coli* XL1-Blue and BL21 (DE3) strains harboring designated vectors were cultured in LB medium supplemented with 0.1 mg/ml ampicillin. All the plasmids used as templates for PCR were extracted by using the plasmid extraction kit (QIAprep Spin Miniprep kit, QIAGEN). All PCR primers were synthesized by BGI Company (Guangdong, China). The *mdh* gene was amplified by PCR using *E. coli* MG1655 chromosomal DNA as a template. The primers contain AgeI and EcoRI restriction sites at the 5'- and 3'-end respectively. The corresponding amplified products were digested with AgeI and EcoRI and ligated into the pHisSUMO plasmid,[1] which has been digested with the same restriction enzymes. The generated plasmid pHisSUMO-*mdh* was extracted and transformed into BL21 (DE3) cells for protein expression.

Protein expression and purification

Overnight cultures of BL21(DE3) cells harboring pHisSUMO-*mdh* were diluted by 1:100 to fresh LB medium supplemented with 0.1 mg/ml ampicillin. Cells were grown at 37 ^{o}C with rotation of 200 rpm until OD_{600} reached 0.6. MDH expression was induced by addition of isopropyl-β-D-thiogalactoside (IPTG) to a final concentration of 500 μM. The bacteria were further incubated at 37 ^{o}C for 3 h and then harvested by centrifugation (5, 000 g, 20 min at 4 ^{o}C). The cell pellets were resuspended in Tris-HNO_3 buffer (50 mM Tris-HNO_3 buffer, 150 mM $NaNO_3$, pH = 7.4) and lysed by sonication. The lysates were centrifuged at 15, 000 g for 30 min, and the supernatant was collected and then applied to a 5 ml HisTrap Q column (GE Healthcare). The proteins were eluted with 300 mM imidazole in Tris-HNO_3 buffer. The eluted proteins were further subjected to SUMO protease (50 NIH units) cleavage at 25 ^{o}C for 2 h to remove the His_6-tag and further purified by HiLoad 16/60 Superdex 200 column equilibrated with Tris-HNO_3 buffer. Plasmids for MDH^{C109S}, MDH^{C113S}, MDH^{C251S}, $MDH^{C109S/C113S}$, $MDH^{C109S/C251S}$, $MDH^{C113S/C251S}$, MDH^{3CS}, $MDH^{3CS/M227S}$, and $MDH^{3CS/H177S}$ mutants were generated via site-directed mutagenesis using Phusion high fidelity DNA polymerase (NEB). The wide-type (WT) pHisSUMO-*mdh* plasmid was used as a DNA template and the site-directed mutations were verified by DNA sequencing (BGI). The primers used for mutants are listed in Table S2. The conditions and steps for expression and purification of MDH mutants were identical to wild-type MDH.

MALDI-TOF MS analysis

Matrix Assisted Laser Ionization Time-of-Flight Mass Spectrometry (MALDI-TOF MS) (Bruker ultraflex extreme MALDI-TOF-TOF-MS) was utilized to monitor the silver binding capability of MDH and its mutants. In brief, saturated sinapic acid

in 1:1 ACN:H_2O was prepared as the matrix. Wild-type MDH, MDH^{3CS}, $MDH^{3CS/M227S}$, and $MDH^{3CS/H177S}$ were incubated with different molar equivalents of Ag^+ at room temperature for 1 h. Proteins at the concentration of 10 μM was mixed with equal volume of matrix and followed with crystalization on polished 384 well plate prior to MALDI-TOF MS analysis. Mass spectra were measured in the positive linear mode.

Isothermal titration calorimetry

The MDH, MDH^{C109S}, MDH^{C113S}, MDH^{C251S} and MDH^{3CS} were prepared in Tris-HNO_3 buffer (35 mM Tris-HNO_3 buffer, 100 mM $NaNO_3$, pH = 7.4) to a final concentration of 24 μM. $AgNO_3$ at the concentration of 720 μM in Tris-HNO_3 buffer was prepared as the titrant. Generally, 40 μl $AgNO_3$ was titrated into 200 μl protein solution with 90 s interval between each injection. The signals of $AgNO_3$ titration into Tris-HNO_3 buffer were recorded as background. All the ITC experiments were performed on a Malvern MicroCal ITC200 at 25 ^oC. All data were analyzed and fitted by one or two set of sites binding models by the Origin software.

GE-ICP-MS

The GE-ICP-MS experiment was performed according to our previous study.[2] In brief, a reverse multilayer native resolving gel (13%→10% with lengths of 1.4 and 2.0 cm respectively) and 4% stacking gel of 0.6 cm were utilized to resolve proteins. A two-step procedure with 200 V (60 min) for protein stacking and 600 V for resolving was applied. At the beginning of the second step, ICP-MS detection was started for elemental detection. The conditions for GE-ICP-MS were kept the same for all experiments. ^{127}I-labelled proteins were added as internal standards for MW calibration.

Enzyme inhibition assay

Freshly prepared MDHs at concentration of 4 nM in Tris-HNO_3 buffer (35 mM Tris-HNO_3 buffer, 100 mM $NaNO_3$, pH = 7.4) were incubated with 12 and 24 nM Ag^+ for 1 h at room temperature. The protein mixtures were further diluted to a final concentration of 4 nM for the measurement of enzyme activities by Malate Dehydrogenase Activity Assay Kit (ab183305). The absorbance at 450 nm was monitored constantly for a duration of 20 min. A standard curve was constructed using five concentrations of NADH ranging from 25 to 500 nmol for calculation. The activity of untreated MDH was set as 100%.

For the test of MDH mutants, freshly prepared WT MDH, MDH^{C109S}, MDH^{C113S}, MDH^{C251S}, MDH^{H177S}, and MDH^{M227S} were further diluted to a final concentration of 4 nM for the measurement of enzyme activities by the standard assay kit. The activity of WT MDH was set as 100%.

X-ray crystallography

Crystals of the apo-MDH were grown by sitting-drop vapor diffusion method with the precipitant containing 0.1 M Tris-HNO_3 (pH 7.5) and 25% PEG 3350 (w/v). Tetragonal crystals appeared within three days and grew up to full size within one week. The crystals were soaked into cryo-protectant solution (0.1 M Tris-HNO_3 pH 7.5, 25% PEG 3350, 2 mM $AgNO_3$ and 20% glycerol) for various time duration before cryo-cooled. The diffraction data were collected at BL17U beamline of Shanghai Synchrotron Radiation Facility (SSRF). For crystals in each condition, at least three sets of data from independent crystals were collected.[3] The diffraction data were processed with XDS.[4] The CCP4 suite[5] and Phenix[6] were used for data refinement and finalization. An apo-MDH structure (PDB code: 1IB6) were used as a model for molecular replacement.[7] TLS refinement was used in the later stage of data processing.

Statistical analysis

Unless specified, all experiments were subjected to three biological replicates and two technique replicates. A two-tailed t-test was used for all comparisons between two groups. Data are presented as mean ± SEM. **P* < 0.05, ***P* < 0.01 and ****P* < 0.001. NS, not significant (*P* > 0.05).

Supplementary Tables

Table S1. Strains, plasmids for protein expression.

Strains	**Application**
XL1-Blue	Plasmid maintenance
BL21(DE_3)	Protein expression
Plasmids	
pHisSUMO	
pHisSUMO-*mdh*	Wild-type MDH protein expression
pHisSUMO-*mdh* ^{C109S}	MDH^{C109S} mutant protein expression
pHisSUMO-*mdh* ^{C113S}	MDH^{C113S} mutant protein expression
pHisSUMO-*mdh* ^{C251S}	MDH^{C251S} mutant protein expression
pHisSUMO-*mdh* ^{H177S}	MDH^{H177S} mutant protein expression
pHisSUMO-*mdh* ^{M227S}	MDH^{M227S} mutant protein expression
pHisSUMO-*mdh* ^{3CS}	MDH^{3CS} mutant protein expression
pHisSUMO-*mdh* $^{3CS/M227S}$	$MDH^{3CS/M227S}$ mutant protein expression
pHisSUMO-*mdh* $^{3CS/H177S}$	$MDH^{3CS/H177S}$ mutant protein expression

Table S2. Primers for plasmid construction.

	Forward Primers (AgeI)	**Reverse Primers (EcoRI)**
MDH	ATTCACCGGTGGAGGAGGTTCCGGAGGTG GAATGAAAGTCGCAGTCCTCG	CCGGAATTCTTACTTATTAACGAACTC
MDH^{C109S}	TGCGAAAACCAGCCCGAAAGCGTGCATTG	CGCTTTCGGGCTGGTTTTCGCAACTTG
MDH^{C113S}	CCCGAAAGCGAGCATTGGTATTATCACT	TAATACCAATGCTCGCTTTCGGGCAGGT
MDH^{C251S}	CGTTGTCGAAAGCGCCTACGTTGAAGGC	CAACGTAGGCGCTTTCGACAACGCCTTG
MDH^{M227S}	CGGTGGCGGGTCTGCAACCCTGTCTAGCG GCCA	GACCAAAACGTGCAGCTGCCTGGCCGCTA GACA
MDH^{H177S}	TATTGGCGGTAGCTCTGGTGTTACCATT	TAACACCAGAGCTACCGCCAATAACCGG

Table S3. Summary of isothermal titration calorimetry data.

Protein	Ligand	N	K_d (μM)	ΔH (kcal mol^{-1})	ΔS (cal mol^{-1} k)
MDH	Ag^+	$N_1 = 1.26 \pm 0.16$	$K_{d1} = 0.25 \pm 0.09$	$\Delta H_1 = -10.02 \pm 0.58$	$\Delta S_1 = -3.38$
		$N_2 = 2.46 \pm 0.12$	$K_{d2} = 5.92 \pm 1.73$	$\Delta H_2 = -6.38 \pm 1.08$	$\Delta S_2 = 2.50$
MDH^{C109S}	Ag^+	$N_1 = 0.97 \pm 0.02$	$K_{d1} = 0.15 \pm 0.04$	$\Delta H_1 = -11.3 \pm 0.51$	$\Delta S_1 = -6.67$
		$N_2 = 1.44 \pm 0.12$	$K_{d2} = 4.20 \pm 1.17$	$\Delta H_2 = -2.80 \pm 0.31$	$\Delta S_2 = 15.2$
MDH^{C113S}	Ag^+	$N = 2.34 \pm 0.12$	$K_d = 9.71 \pm 2.95$	$\Delta H = -4.64 \pm 0.34$	$\Delta S_2 = 7.39$
MDH^{C251S}	Ag^+	$N_1 = 0.94 \pm 0.02$	$K_{d1} = 0.17 \pm 0.08$	$\Delta H_1 = -13.2 \pm 0.33$	$\Delta S_1 = -13.4$
		$N_2 = 1.04 \pm 0.10$	$K_{d2} = 3.13 \pm 0.11$	$\Delta H_2 = 5.72 \pm 1.04$	$\Delta S_2 = 44.4$
MDH^{3CS}	Ag^+	Not detectable			

Table S4. Summary of X-ray crystallography data collection and refinement statistics.*

Data collection	**Apo MDH**	**Ag-MDH-1**	**Ag-MDH-2**	**Ag-MDH-3**
PDB ID	**6KA1**	**5Z3W**	**7CGC**	**7CGD**
Wavelength (Å)	1.04008	0.97914	0.97914	0.97914
Resolution range (Å)	33.01 - 1.54 (1.60 - 1.54)	38.83 - 2.29 (2.37 - 2.29)	40.71 - 2.55 (2.63 - 2.55)	40.72 - 2.06 (2.13 - 2.06)
Space group	$P2_1$	$P2_1$	$P2_1$	$P2_1$
a, b, c (Å)	57.93, 125.10, 85.76	57.65, 124.56, 85.50	58.222, 128.129, 85.195	57.64, 124.68, 85.15
α, β, γ (º)	90.00, 107.12, 90.00	90.00, 107.10, 90.00	90.00, 107.10, 90.00	90.00, 106.99, 90.00
Unique reflections	157580 (14412)	50964 (5108)	37330 (3764)	69971 (7055)
Completeness (%)	92.19 (84.39)	98.23 (98.76)	97.94 (99.47)	98.56 (99.17)
Mean I/sigma(I)	20.9 (4.3)	18.5 (12.7)	11.9 (8.2)	15.8 (7.6)
Wilson B-factor	12.52	24.40	30.38	23.65
R-merge	0.00148 (0.687)	0.0506 (0.0611)	0.135 (0.245)	0.0594 (0.126)
R-meas	0.00209 (0.743)	0.07167 (0.0865)	0.191 (0.346)	0.0840 (0.178)
Reflections for refinement	157579 (14412)	50959 (5108)	37323 (3763)	69953 (7052)
R-work	0.156 (0.184)	0.206 (0.247)	0.244 (0.291)	0.215 (0.243)
R-free	0.182 (0.226)	0.230 (0.289)	0.291 (0.395)	0.245 (0.289)
Number of non-hydrogen atoms	9898	8748	8728	8818
RMSD (bonds) (Å)	0.005	0.002	0.003	0.002
RMSD (angles) (º)	0.80	0.49	0.51	0.51
Ramachandran favoured (%)	99.75	99.49	98.14	98.65
Ramachandran allowed (%)	0.25	0.51	1.69	1.35
Ramachandran outliers (%)	0.00	0.00	0.17	0.00

*Statistics for the highest-resolution shell are shown in parentheses.

Ag-MDH-1, Ag-MDH-2, and Ag-MDH-3 crystals are soaked with 2 mM Ag^+ for 10 min, 30 min, and 1 h respectively.

Table S5. Positive peaks in the m*F*o-D*F*c map of Ag-MDH-1, Ag-MDH-2 and Ag-MDH-3.*

Corresponding Atom	Peak Height (σ)	Structure
Ag401	24.5	Ag-MDH-1
Ag401	22.2**	Ag-MDH-2
Ag402	27.4	Ag-MDH-2
Ag403	23.5	Ag-MDH-2
Ag404	18.9	Ag-MDH-2
Ag401	32.8	Ag-MDH-3
Ag402	27.4	Ag-MDH-3
Ag403	42.2	Ag-MDH-3
Ag404	29.1	Ag-MDH-3
Ag405	24.1**	Ag-MDH-3
Ag406	22.1**	Ag-MDH-3
Ag407	24.6**	Ag-MDH-3

*The search was based on the final model with all or some silver atoms removed from Chain A.

**Calculated after other silver atoms in Chain A listed in the table were picked up.

Table S6. Metal-ligand distances (Å) in Ag-MDH-1 and Ag-MDH-2 structures.*

Metal	Ligand	Distance (Å)
Ag-MDH-1		
Ag401	Cys113-Sγ	2.6
Ag401	HOH515	2.6
Ag-MDH-2		
Ag401	Cys113-Sγ	2.8
Ag401	HOH502	2.8
Ag402	Cys113-Sγ	2.5
Ag402	Lys142-Nζ	2.2
Ag401	Ag402	2.7
Ag403	Cys251-Sγ	2.3
Ag403	Val173-N	2.2
Ag403	Val173-O	2.7
Ag404	Cys251-Sγ	2.8
Ag404	HOH504	2.9
Ag403	Ag404	3.2

*The measurements are made on the atomic coordinates of Chain A of both structures.

Table S7. Ligand-Ag-ligand angles (º) in Ag-MDH-1 and Ag-MDH-2 structures.*

Atom1	Atom2	Atom3	Angle (º)
Ag-MDH-1			
Cys113-Sγ	Ag401	HOH515	159.1
Ag-MDH-2			
Cys113-Sγ	Ag401	HOH502	153.8
Cys113-Sγ	Ag402	Lys142-Nζ	164.1
Cys251-Sγ	Ag403	Lys173-N	153.8
Cys251-Sγ	Ag404	HOH504	131.3

* The measurements are based on the atomic coordinates of Chain A.

Supplementary Figures

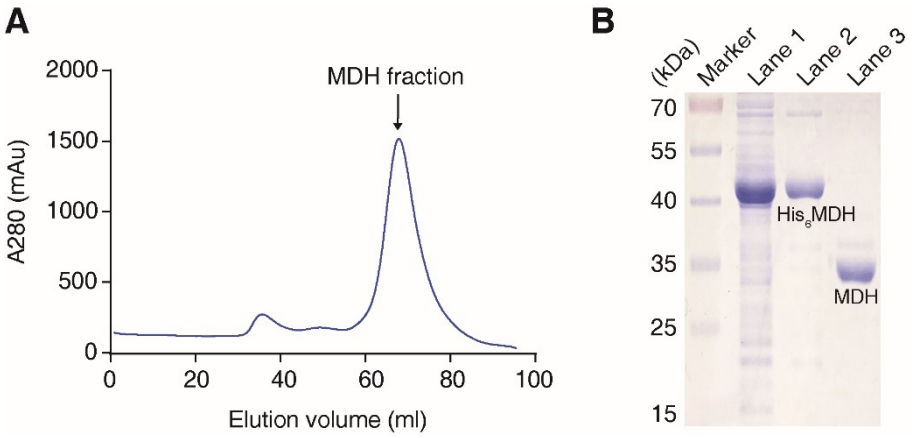

Figure S1. Overexpression and purification of MDH. (A) Purity of MDH confirmed by gel filtration on a column Hiload 16/60 Superdex 200 (GE Healthcare) pre-equilibrated with 35 mM Tris-HNO_3, 100 mM $NaNO_3$, pH = 7.4. (B) Purity of MDH confirmed by SDS-PAGE. Lane 1, whole cell lysate. Lane 2, His_6-MDH. Lane 3, purified MDH.

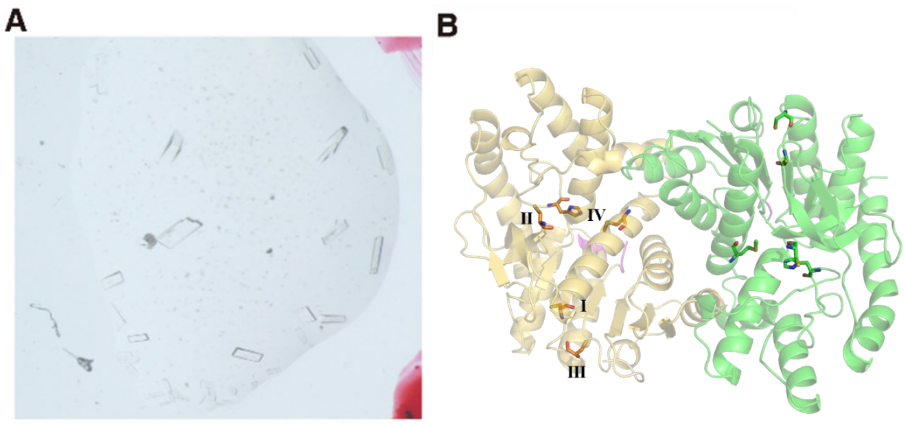

Figure S2. Crystals and structure of apo-MDH. (A) The picture of apo-MDH crystals. (B) The overall structure of apo-MDH in cartoon representation with two monomers are shown. The residues near the disordered active site loop are shown in violet. The four silver binding sites are highlighted in sticks.

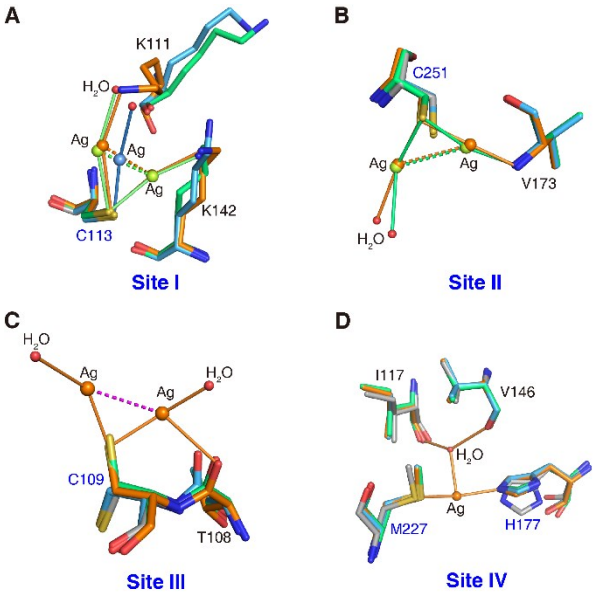

Figure S3. Comparison of Ag^{+} coordination geometry at different sites. The overlay of Cys113 site (A), Cys251 site (B), Cys109 site (C), and Met227/His177 (D) site of apo-MDH (Grey), Ag-MDH-1 (Blue), Ag-MDH-2 (Green) and Ag-MDH-3 (Orange) are shown. Structural alignment was done over C_{α} residues.

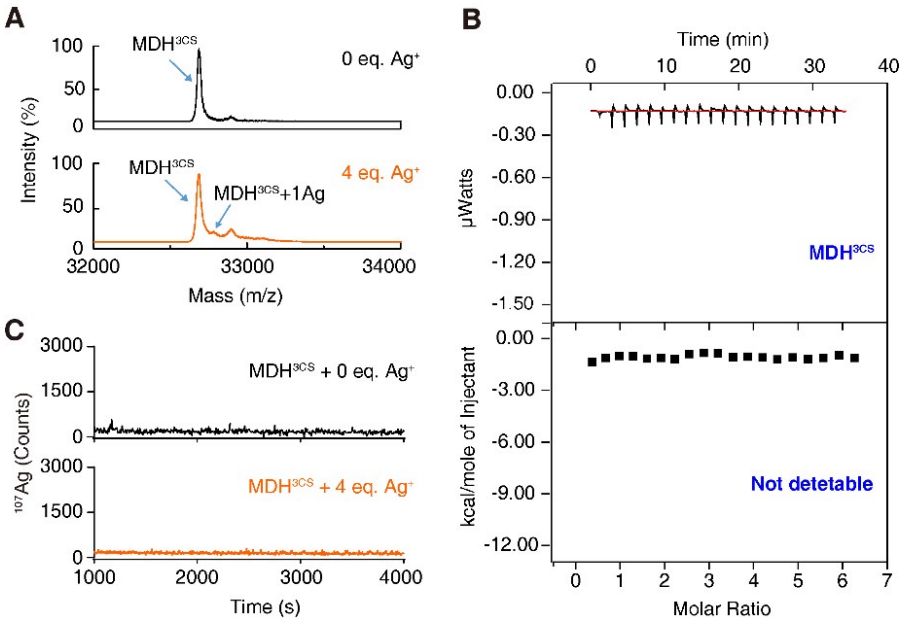

Figure S4. The effect of site-directed multiple mutations on the silver binding capability of MDH. (A) MALDI-TOF mass spectra of MDH^{3CS} with or without incubation of Ag^+. (B) ITC result of Ag^+ binding to MDH^{3CS}. (C) GE-ICP-MS electropherograms (^{107}Ag) of MDH^{3CS} with or without treatment of Ag^+. All experiments were performed in triplicate. One representative of three replicates is shown (A, B, C).

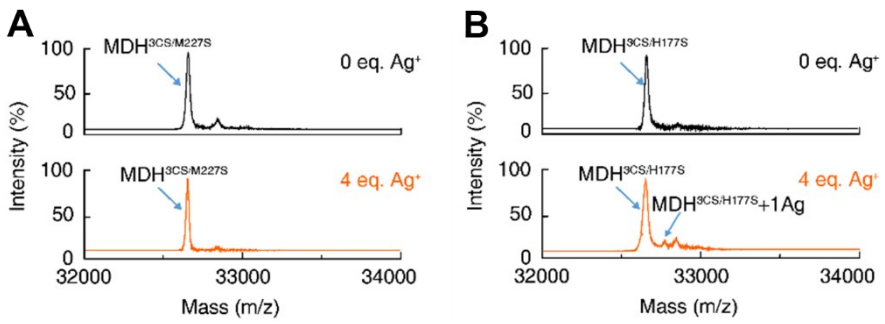

Figure S5. The effect of site-directed multiple mutations on the silver binding capability of MDH. (A) MALDI-TOF mass spectra of $MDH^{3CS/M227S}$ with or without incubation of Ag^{+}. (B) MALDI-TOF mass spectra of $MDH^{3CS/H177S}$ with or without incubation of Ag^{+}. All experiments were performed in triplicate. One representative of three replicates is shown (A, B).

References

1. Fong, Y. H.; Wong, H. C.; Yuen, M. H.; Lau, P. H.; Chen, Y. W.; Wong, K. B., Structure of UreG/UreF/UreH complex reveals how urease accessory proteins facilitate maturation of *Helicobacter pylori* urease. *PLoS Biol.,* **2013,** *11*, e1001678.
2. Hu, L.; Cheng, T.; He, B.; Li, L.; Wang, Y.; Lai, Y.-T.; Jiang, G.; Sun, H., Identification of metal-associated proteins in cells by using continuous-flow gel electrophoresis and inductively coupled plasma mass spectrometry. *Angew. Chem. Int. Ed.,* **2013,** *52*, 4916-4920.
3. Wang, Q.-S.; Zhang, K.-H.; Cui, Y.; Wang, Z.-J.; Pan, Q.-Y.; Liu, K.; Sun, B.; Zhou, H.; Li, M.-J.; Xu, Q.; Xu, C.-Y.; Yu, F.; He, J.-H., Upgrade of macromolecular crystallography beamline BL17U1 at SSRF. *Nucl. Sci. Tech.,* **2018,** *29*, 68.
4. Kabsch, W., XDS. *Acta. Crystallogr. D.,* **2010,** *66*, 125-132.
5. Collaborative, The CCP4 suite: programs for protein crystallography. *Acta. Crystallogr. D.,* **1994,** *50* (5), 760-763.
6. Adams, P. D.; Afonine, P. V.; Bunkoczi, G.; Chen, V. B.; Davis, I. W.; Echols, N.; Headd, J. J.; Hung, L.-W.; Kapral, G. J.; Grosse-Kunstleve, R. W.; McCoy, A. J.; Moriarty, N. W.; Oeffner, R.; Read, R. J.; Richardson, D. C.; Richardson, J. S.; Terwilliger, T. C.; Zwart, P. H., PHENIX: a comprehensive Python-based system for macromolecular structure solution. *Acta. Crystallogr. D.,* **2010,** *66*, 213-221.
7. McCoy, A. J.; Grosse-Kunstleve, R. W.; Adams, P. D.; Winn, M. D.; Storoni, L. C.; Read, R. J., Phaser crystallographic software. *J. Appl. Crystallogr.,* **2007,** *40*, 658-674.